Reduced enteric BDNF-TrkB signaling drives glucocorticoid-mediated GI dysmotility

Jared Slosberg[1#], Srinivas N. Puttapaka[2#], Philippa Seika[2], Su Min Hong[2], Alpana Singh[3], Subhash Kulkarni[2, 5, 6*]

[1]Department of Genetic Medicine, Johns Hopkins University – School of Medicine, Baltimore, MD, USA

[2]Division of Gastroenterology, Dept of Medicine, Beth Israel Deaconess Medical Center, Boston, MA 02115

[3]Cleveland Clinic, Cleveland

[4]Department of Oncology, Johns Hopkins University – School of Medicine, Baltimore, MD, USA

[5]Division of Medical Sciences, Harvard Medical School, Boston, MA 02115

[6]Graduate program in Neuroscience, Harvard Medical School, Boston, MA 02115

[#]Joint first co-authors

*Address all correspondence to:

Subhash Kulkarni, Ph.D.

skulkar1@bidmc.harvard.edu

Abstract:

Stress affects gastrointestinal (GI) function causing dysmotility, especially in *disorders of gut-brain interactions (DGBI)* patients. GI motility is regulated by the enteric nervous system (ENS), suggesting that stress alters ENS biology to cause dysmotility. While stress increases glucocorticoid levels through the hypothalamus-pituitary-adrenal axis, how glucocorticoids affect GI motility is not known. Glucocorticoid signaling reduces expression of specific transcriptional isoforms of brain-derived neurotrophic factor (BDNF) in the central nervous system, altering signaling through its receptor Tropomyosin-related kinase B (TrkB) to cause behavioral defects. However, since the nature of ENS-specific *Bdnf* isoforms and their response to glucocorticoids remains unknown, we are limited in studying how stress impacts the ENS to cause dysmotility. Here, in male and female mice, we establish that stress-responsive *Bdnf* isoforms that are transcriptionally regulated at exons 4 and 6 represent >85% of all *Bdnf* isoforms in the post-natal ENS, and that *Bdnf* and *Ntrk2* (TrkB) are expressed by enteric neurons. We further show using male mice dosed with a synthetic glucocorticoid receptor (GR) agonist dexamethasone (Dexa), that increased glucocorticoid signaling in ENS significantly reduces the expression of *Bdnf* transcripts and protein and that it significantly reduces GI motility. Finally, by using HIOC, a specific synthetic agonist of TrkB, we observe that HIOC treatment significantly improved GI motility of a cohort of Dexa-treated male mice, when compared to Dexa-treated and HIOC-untreated mice. Our results implicate BDNF- TrkB signaling in the etiology of stress-associated dysmotility and suggest that TrkB is a putative therapeutic target for dysmotility in DGBI patients.

43 **Significance statement:**

44 The mechanism through which stress-associated increase in glucocorticoid signaling causes
45 gastrointestinal (GI) dysmotility is not well understood. GI motility is regulated by the enteric
46 nervous system, which depends on optimal signaling between brain-derived neurotrophic factor
47 (BDNF) and its receptor tropomyosin related kinase B (TrkB). The lack of clarity on whether
48 glucocorticoid impact BDNF signaling in the ENS, analogous to the manner they affect BDNF in
49 brain, has limited our understanding of stress-associated dysmotility. Here, by identifying the
50 nature of *Bdnf* isoforms expressed in ENS, studying their response to increased glucocorticoid
51 signaling, and testing the effect of TrkB agonist to promote healthy gut motility in a model of
52 glucocorticoid-driven dysmotility, we implicate altered BDNF-TrkB signaling as the mechanism
53 driving stress-associated dysmotility.

54 **Introduction:**

55 Stress-associated gastrointestinal (GI) dysmotility afflicts large numbers of patients and is an
56 important factor in the development of irritable bowel syndrome (IBS) (Qin et al., 2014; Sperber
57 et al., 2021; Leigh et al., 2023). GI motility is regulated by the enteric nervous system (ENS)
58 (Wood, 2016), suggesting that stress-associated GI dysmotility occurs due to ENS dysfunction.
59 Healthy ENS function relies on optimal neurotrophin signaling, which include interactions between
60 neurotrophins, which are secreted by diverse gut cell types, and their specific receptor that is
61 expressed by ENS neurons (Liu, 2018; Chalazonitis et al., 2020; Sharkey and Mawe, 2023).
62 Brain-derived neurotrophic factor (BDNF) and its receptor tropomyosin kinase B (TrkB, coded by
63 *Ntrk2*) constitutes one such significant neurotrophin system known to regulate neuronal signaling
64 in the central nervous system (CNS) (Martinowich et al., 2007). Stress also causes significant
65 changes in CNS neuronal function resulting in significant and observable changes in behavior
66 (Zheng et al., 2024), and stress-induced reductions in BDNF expression and hence BDNF–TrkB
67 signaling is known to be a significant mechanism through which stress affects CNS function
68 (Begni et al., 2016). However, whether a similar BDNF-dependent mechanism drives stress-
69 associated GI dysmotility is not known.
70
71 Studies on rodent models of health and disease have informed that BDNF regulates GI motility
72 as its presence accelerates gastrointestinal transit, likely through a combination of its
73 neuromodulatory role and more direct effects on the excitatory potential of the muscularis externa
74 (Boesmans et al., 2008; Chen et al., 2012; Chen et al., 2014; Singh et al., 2020). This prokinetic
75 effect of BDNF observed in rodents appears to translate to slow-transit constipation (STC)
76 patients, as decreased BDNF presence was detected in colonic tissues from this cohort (Chen et
77 al., 2014) and exogenous BDNF supplementation restored intestinal transit measures in
78 constipated patients (Coulie et al., 2000). These data suggest that mechanisms regulating BDNF
79 levels are important for the pathobiology of GI dysmotility. Further, significant alterations in *Bdnf*
80 transcript levels in distressed IBS patients (Konturek et al., 2020; Zhang et al., 2021) suggest that
81 this regulation may extend to stress-induced GI dysmotility. However, how stress affects enteric
82 BDNF and TrkB and if stress-induced reduction in enteric BDNF levels and BDNF–TrkB signaling
83 mediate the development of GI dysmotility is not known.

84 BDNF levels are regulated at the level of transcription. The *Bdnf* gene consists of nine exons of
85 which the first 8 are non-coding exons (e1 – e8) that are transcribed but not translated, and only
86 the 9th exon (e9) contains the translated coding sequence (Aid et al., 2007). Transcription results

87 in *Bdnf* isoforms containing any one of the eight e1 – e8 exons spliced to the protein coding exon
88 e9. The non-coding exons each provide alternative transcription start sites for *Bdnf* isoforms, and
89 each non-coding exon contains an exon-specific promoter sequence that is differentially regulated
90 (Aid et al., 2007). Variation in promoter usage allows for context-dependent regulation of *Bdnf*
91 expression, as has been demonstrated for activity-dependent synaptic plasticity in the CNS (Hong
92 et al., 2008; Pruunsild et al., 2011). Additionally, physiological stress has been implicated as a
93 potent regulator of *Bdnf* expression and abundance (Murakami et al., 2005; Tsankova et al., 2006;
94 Hill and Martinowich, 2016; Linz et al., 2019). Stress manifests its many effects on viscera through
95 the hypothalamic-pituitary-adrenal (HPA) axis, whereby corticotropin-releasing hormone (CRH)
96 released by hypothalamic neurons in response to stress induces the release of
97 adrenocorticotropic hormone (ACTH) from pituitary. This, in turn, directs the adrenal glands to
98 release the glucocorticoid hormone cortisol (Russell and Lightman, 2019). Chen et al.(Chen et
99 al., 2017) observed that Glucocorticoids (GCs) specifically repress the expression of *Bdnf*
100 isoforms IV (transcription from promoter of *Bdnf*-e4) and VI (transcription from promoter of *Bdnf*-
101 e6) by binding to the glucocorticoid responsive elements (GREs) in e4 and e6 promoter
102 sequences. While the effect of both stress and glucocorticoid supplementation on altering gut
103 motility in adult mice has been observed (Schneider et al., 2023), whether stress-associated GI
104 dysmotility is driven by a similar glucocorticoid-mediated repression of *Bdnf* in the ENS is not
105 known. This lack of understanding has been driven by a lack of clarity on the nature of BDNF and
106 TrkB-expressing cells in the gut wall, the nature of *Bdnf* isoform expression and their susceptibility
107 to glucocorticoid stimulation in the adult ENS, and whether stimulating TrkB signaling reverts the
108 effect of glucocorticoid-induced GI dysmotility.

109 To address these gaps in the field, here, we further our mechanistic understanding of stress-
110 associated GI dysmotility by using immunofluorescence, RNAScope, bulk transcriptomic, and
111 quantitative PCR-based assays to study the expression of BDNF and TrkB in the gut wall tissue
112 containing myenteric neurons. Further, we used restraint stress and a synthetic glucocorticoid
113 receptor agonist Dexamethasone to assess how stress and glucocorticoid receptor stimulation
114 influence BDNF levels to drive dysmotility. Finally, we test whether stimulating BDNF-TrkB
115 signaling promotes healthy GI motility in a mouse model of glucocorticoid-induced GI dysmotility.
116 Our results show that both BDNF and TrkB are expressed by adult enteric neurons, and that
117 stress-responsive isoforms of *Bdnf* represent the majority of all *Bdnf* isoforms in the post-natal
118 myenteric plexus tissue. We find that dexamethasone exposure causes a significant reduction in
119 BDNF protein levels, driven by a significant reduction in expression of the stress-responsive *Bdnf*

120 isoforms, and that dexamethasone-induced abnormalities in GI motility can be reversed by
121 stimulating TrkB signaling using a specific TrkB agonist HIOC.

122 **Methods**

123 Human tissue procurement and immunohistochemistry: Paraffin sections of the adult small
124 intestinal full-thickness gut from deidentified human tissues were obtained from the Department
125 of Pathology at Beth Israel Deaconess Medical Center, and the Institutional Review Board
126 approved using the deidentified human tissues. Antigen retrieval was performed on 5 um thick
127 sections at 97ºC for 40 minutes using citrate buffer at pH 6.0, followed by immunostaining with
128 anti-BDNF antibody (abcam, Cat. No. ab108319, dilution 1:500). The tissue sections were then
129 counterstained with DAB chromogen staining, mounted with Cytoseal, and imaged under 40X
130 brightfield. Microscopy was performed using the Nikon Eclipse Ni-U Upright microscope with 40x
131 Nikon Plan Fluor objective. Images were acquired using the Nikon DS-Fi3 camera and NIS-
132 Elements BR software (Version 5.20.01). During image acquisition, exposure time was adjusted
133 using the Color DS-Fi3 settings to obtain a clear definition of tissue structure. Images were
134 acquired in the TIFF format.

135 Animals: We used male and female wildtype C57BL/6J mice from the National Institute on Aging
136 colony (at the ages of 1, 6, and 17 months) for the bulk RNA sequencing experiment. For all other
137 experiments, we used adult male wildtype C57BL/6J mice (between the ages of 12 and 20 weeks)
138 from the National Institute on Aging colony. Mice were housed in a controlled environment under
139 a 12 h light/dark cycle at 22 ± 2℃, 55 ± 5% humidity with access to food and water ad libitum. All
140 animal procedures were carried out strictly under protocols approved by the Animal Care and Use
141 Committee of Johns Hopkins University and of Beth Israel Deaconess Medical Center (BIDMC)
142 in accordance with the guidelines provided by the National Institutes of Health.

143 Bulk RNA sequencing (bulkRNA-seq) experiments:

144 *Tissue Isolation for bulkRNA-seq:* Mice of three ages (1-month, 6-month, and 17-month) and both
145 sexes (n=3 per unique condition) were anesthetized with isoflurane and sacrificed by cervical
146 dislocation. For small intestinal tissue isolation, a laparotomy was performed, and the entire small
147 intestine was removed and flushed with ice-cold nuclease-free 1X PBS. The ileum, defined as the
148 distal third of the small intestine, was cut into 3 cm sections for peeling. Next, tissues were placed
149 over a sterile plastic rod and a superficial longitudinal incision was made along the serosal surface
150 and the longitudinal muscle containing myenteric plexus (LM-MP) was peeled off from the
151 underlying tissue using a wet sterile cotton swab. Each gut muscle strip was immediately flash

152 frozen in liquid nitrogen before storage at -80°C. The average time from sacrifice to flash freeze
153 was 10 minutes. Animals were processed in three batches, balanced across age/sex composition
154 and order of processing.

155 *Library Prep & Sequencing:* RNA isolation, library preparation, and sequencing were completed
156 at the JHU Single Cell and Transcriptomic Core. Samples with RIN >= 7.0 were used for library
157 preparation, with all samples being high-quality except one 17-month female (resulting n=2,
158 average RIN of 17 samples that passed this threshold > 9.0). Frozen tissue samples each in
159 1.5mL tubes were submerged in 375 uL of RLT buffer with β-mercaptoethanol. Tissue and buffer
160 were transferred to a ice-cold 2 mL Qiagen sample tube with a 5mm stainless steel bead and
161 lysed in a TissueLyzer at full speed for 3 minutes. RNA isolation was completed with the Qiagen
162 RNeasy Mini, Animal Tissue and Cells with DNA Digest protocol. cDNA libraries were prepared
163 with the TruSeq Stranded mRNA Library Prep with unique dual indexes. Paired-end (2x-50bp)
164 sequencing was completed on a NovaSeq 6000 system.

165 *Preprocessing*: Isoform-level transcript abundances were estimated by pseudoalignment via
166 Kallisto 'quant' (version 0.48.0) to the GENCODE vM27 reference genome assembly. Default
167 parameters were used, except the number of bootstraps was set to 100 to estimate uncertainty
168 ("-b 100"). The median fragment length, as estimated by Kallisto, was 168.7 base pairs. Across
169 all sequenced samples, the median number of reads per sample was 46,756,241 (range: 34.6 M
170 to 58.2 M) and 94.2% of reads were successfully pseudoaligned to the reference.

171 *Quality control & analysis:* For quality control analyses, isoforms were collapsed to gene-level
172 and abundances were normalized by the "scaledTPM" option within tximport, and further analyzed
173 with DESeq2 (v1.30.1, R v4.0.2). Genes were removed from the analysis if they had fewer than
174 10 counts across all samples or were not detected in at least three samples. At the sample level,
175 PCA and Cook's distance were used to identify potential outliers. Both approaches identified one
176 17-month male sample as a source of outlier expression, and this sample also had the lowest
177 RIN (7.0). With this outlier sample removed, isoform-level abundances of the remaining 16
178 samples were analyzed with IsoformSwitchAnalyzeR (v2.1.2, R v4.2).

179 Restraint stress model: Adult male mice were divided into two cohorts, control and stressed. Mice
180 in stressed cohorts were restrained for 1 hour every day for 5 consecutive days and were then
181 released back into their cages. The timing of the restraint during the day was varied across the 5
182 days to reduce habituation. By contrast, the mice in the control group were handled similarly, but
183 were not restrained and were returned to the cage immediately after handling. The whole gut

184 transit time (WGTT) of the mice in response to treatment was assayed on the day after the last
185 day of restraint.

186 Dexamethasone induced model of GI dysmotility: Adult male mice were divided into two cohorts,
187 control and DEXA. Mice in the control group were treated with vehicle (10% DMSO in saline,
188 intraperitoneal route) and those in the DEXA group were treated with dexamethasone
189 (MedChemExpress, Cat. No. HY-14648; 5mg/kg in 10% DMSO/body weight, intraperitoneal
190 route) group. Dexamethasone is light sensitive so was shielded from bright light, both in powder
191 form and in solution. Mice were first housed in individual cages and after a habituation phase
192 lasting 30min, they were treated with vehicle or dexamethasone, which were administered
193 intraperitoneally using a sterile 1 ml insulin syringe. The mice were subjected to WGTT assays
194 30 minutes after the treatment.

195 Another 2 cohorts of mice were similarly used, wherein one the control cohort was dosed similarly
196 with vehicle and the DEXA group was dosed similarly with dexamethasone. 4 hours after the
197 treatment, the mice were sacrificed, and their small intestinal LM-MP tissues were isolated and
198 immediately snap-frozen in liquid nitrogen.

199 Effect of TrkB agonist HIOC on dexamethasone-induced model of GI dysmotility: HIOC (N-[2-(5-
200 hydroxy-1H-indol-3-yl)ethyl]-2-oxopiperidine-3-carboxamide) is a known specific agonist of TrkB.
201 Adult male mice were divided into two cohorts, DEXA and DEXA+HIOC. Mice were first housed
202 in individual cages and then those in the DEXA+HIOC group were treated with HIOC
203 (MedChemExpress, Cat. No. HY-101446; 50 mg/kg in 10% DMSO/body weight, intraperitoneal
204 route), while those in DEXA group were treated with Vehicle (10% DMSO in saline, intraperitoneal
205 route). The mice were then released back to their individual cages for 30 minutes after which both
206 groups were treated with DEXA (50 mg/kg in 10% DMSO/body weight, intraperitoneal route) and
207 again released back to their individual cages for an additional 30 minutes. Treatment was
208 administered intraperitoneally using a sterile 1 ml insulin syringe. The mice were subjected to
209 whole gut transit time assays 30 minutes after the DEXA treatment.

210 Whole gut transit time analyses (WGTT): These experiments were started between the times of
211 8 and 9 AM. Mice were individually caged in plastic cages without bedding and were left
212 undisturbed 30 minutes. Water was provided to the mice before and during the experiment *ad*
213 *libitum*. All mice received oral gavage of 300 µl of 6% (w/v) carmine red (Sigma C1022) in 0.5%
214 (w/v) methylcellulose (Sigma M0512) in sterile water. The oral gavage was performed such that
215 the entirety of the dye suspension was delivered into the animal's stomach. The mice were then

216 left undisturbed in their individual cages for 70 minutes after which their cages were checked
217 every 15 minutes for the presence of red colored fecal pellets. The time post-gavage for every
218 mouse to produce a red colored fecal pellet was measured, and the difference between the
219 gavage time and red fecal pellet production time was established as the whole gut transit time for
220 that mouse. The experiment was terminated at 250 minutes post-gavage and the WGTT of any
221 mice that did not expel the red dye at the termination was marked at the value of 265 (i.e. 250 +
222 15) min. The mean difference in WGTT (in minutes) between cohorts was analyzed statistically.

223 Mouse small intestine LM-MP tissue isolation for non-sequencing experiments: Mice were
224 anesthetized with isoflurane and sacrificed by cervical dislocation. Mouse placed in dorsal
225 recumbency on the surgical surface, disinfected skin with 70% EtOH then opened the abdominal
226 cavity and collected the small intestine (SI) into a petri dish containing PBS with 1x Pen-Strep.
227 Sterile PBS solution flushed through the intestine using a 20ml syringe to remove fecal matter.
228 Entire small intestine cut into 2cm pieces into a sterile petri dish containing Opti-MEM medium
229 with 1X Pen-Strep. SI segments were placed over a sterile 1ml pipette and LM-MP tissue was
230 peeled off from the underlying tissue using a wet sterile cotton swab. Tissues isolated for qPCR-
231 based assessment of *Bdnf* levels were snap frozen immediately after isolation. Tissues isolated
232 for culture were placed in a fresh sterile ice-cold Opti-MEM medium for further use. Tissues
233 isolated for RNAScope analyses were flattened and cryo-preserved in optimal cutting temperature
234 (OCT) compound (TissueTEK) on dry ice.

235 *In Vitro* LM-MP tissue culture and treatments: Isolated LM-MP tissues were placed in a sterile 24
236 well dish containing Stem cell media (SCM, made up of Neurobasal medium containing L-
237 glutamine, B27, and Pen-Strep (all Invitrogen) and Bovine Serum Albumin (Sigma)(Kulkarni et al.,
238 2017)) and treated with Vehicle (10% DMSO in saline) or Dexamethasone (1μM in 10% DMSO)
239 for 4 hrs. After the incubation, tissues were snap frozen in liquid nitrogen & stored at -80°C for
240 further experimental analysis.

241 RNA isolation and quantitative real-time PCR: Total RNA was extracted from frozen LM-MP
242 tissues with Direct-zol RNA miniprep kit (Zymo research) and 1 μg RNA was converted to cDNA
243 using SuperScript III (Therno, Cat.No.11752050) in a 20μl reaction. Quantitative real-time PCR
244 was performed on a QuantStudio3 real time PCR system (Life Technologies, USA) with TaqMan
245 Fast advanced qPCR Master Mix (Cat. No. 4444557, Thermo Scientific, USA) using gene specific
246 TaqMan assay probes. Mouse HPRT served as a housekeeping gene for normalization. Primer
247 and probe information is provided in Table 1. 20μl qRT-PCR reactions were incubated at 95 ℃ for

248 10 min, followed by 40 cycles at 95 ℃ for 10 s, 60℃ for 10 s, and 72 ℃ for 40 s. Relative fold
249 changes of genes between treatment groups were calculated using the $2^{-\Delta\Delta Ct}$ method.

250 Protein isolation and ELISA: Proteins from frozen LM-MP were extracted using a cell lysis buffer
251 containing RIPA buffer (150 mM NaCl, 50 mM Tris-HCl pH 8.0, 1% NP-40, 0.1% sodium
252 deoxycholate and 0.1% SDS, adjusted with distilled water). Succinctly, for every LM-MP peel, we
253 add 20 µl of 1X RIPA+++ buffer which contains RIPA with Halt Protease Inhibitor (Invitrogen, Cat.
254 No. 78438) at a conc. of 5-10X and Phosphatase Inhibitors 2 and 3 (Sigma Aldrich, Cat. Nos.
255 P5726 and P0044) at a concentration of 2-3% to locking sterile Eppendorf tubes and then add 6-
256 8 sterile autoclaved silicon beads. Tissue was homogenized using bead beater in cold room at 7-
257 8 speed setting for 5 mins, after which the tubes were shaken at 200-250 rpm for 30-40 mins in
258 cold room, centrifuged at over 12,000rpm for 20 mins at 4ºC. Supernatant thus generated was
259 collected to be used for ELISA. The levels of BDNF in the LM-MP tissues cultured with and without
260 dexamethasone were measured using the BDNF DuoSet kit (R&D Systems; DY248). In brief,
261 sterile and clean ELISA-grade 96-well (Corning) were coated with 100 µl of diluted capture
262 antibody/well and incubated overnight at room temperature. On the second day, the plates were
263 washed and blocked with reagent diluent (300 µl for 1 hour at room temperature and 100 µl of
264 protein extract, standards in reagent diluent, or appropriate diluent were added to the prepared
265 wells and incubated for 2 hours at room temperature. Following this, 100 µl each of detection
266 antibody, working dilution of streptavidin-HRP, substrate solution, and 50 µl of stop solution were
267 sequentially added to each well. The optical density of each well was measured using a microplate
268 reader set to 540 nm. The BDNF concentration was expressed in picograms of BDNF per
269 microgram of protein.
270 RNAScope: 15 µm thick sections of adult murine small intestinal LM-MP tissues that were fresh
271 frozen in OCT were processed for RNAscope® 2.0 assay for labeling and detecting *Bdnf, Ntrk2*
272 (TrkB) and pan-neuronal *Tubb3* transcripts, which was performed using manufacturer's
273 instructions(Wang et al., 2012). The information on the probes used is provided in Table 1.
274 RNAscope® labeling was provided by the Neurobiology Imaging Facility (NIF) at Harvard Medical
275 School, Boston, MA. The tissue sections after labeling were labeled with DAPI (nuclear dye) and
276 mounted with Prolong Gold Anti-fade mountant (Invitrogen) and imaged under Zeiss 880 Confocal
277 microscope using 40X water immersion objective. The images were analyzed with Fiji (ImageJ,
278 NIH).
279

280

Results

Restraint stress and glucocorticoid receptor agonism in adult mice slows down whole gut motility. The Thaiss group recently studied the effect of restraint stress on GI motility and found that this physiological stress significantly slows down whole GI motility (Schneider et al., 2023). We recreated this model and found concordance with these results, as restraint stress applied in our adult male C57BL/6 mice also caused a significant slowing of whole gut motility, as assayed by the carmine-red dye method (n = 5/cohort; mean ± S.E. of WGTT (in min): Control: 93.0 ± 5.612; Stress: 123.0 ± 8.746, p = 0.02, Students' t-test; **Fig 1**). Since stress manifests its effects through the HPA axis to increase glucocorticoid levels resulting in increased glucocorticoid receptor (GR) agonism, we tested whether a synthetic GR agonist dexamethasone (Dexa) similarly causes a similar slowdown in whole GI motility. Expectedly, mice dosed with Dexa showed a significant delay in their whole GI motility, when compared to vehicle-treated Control mice (n = 5/cohort; mean ± S.E. of WGTT (in min): Control: 145.0 ± 20.12; Dexa: 214.0 ± 17.49, p = 0.03, Students' t-test; **Fig 2**).

Stress-responsive isoform *VI* is the dominant *Bdnf* isoform expressed in the murine longitudinal muscle - myenteric plexus tissue. We first characterized the expression profile of *Bdnf* in the motility-regulating myenteric plexus tissue of post-natal gut across three ages and in the two sexes. We isolated longitudinal muscle and myenteric plexus (LM-MP) tissue from the ileum of juvenile (1 month), adult (6 month), and aging (17 month) male and female mice (n = 3/sex for 1-month and 6-month-old mice, n = 3 males and 2 females for 17-month-old mice) and performed bulk RNA sequencing. First, we confirmed that *Bdnf* transcripts are detected in the ileal tissues of male and female mice at all ages. We next analyzed whether the stress-responsive *Bdnf IV* (from e4) and *Bdnf VI* (from e6) are expressed in the ileal LM-MP tissue across ages and in the two sexes. We found that at all profiled ages, *Bdnf VI* is the dominant isoform, making up 85.3% (95% CI [81.5%, 89.0%]) of all detected *Bdnf* transcripts (**Fig 3**). Similarly, *Bdnf V* (from e5) expression is detected at all ages and in both male and female tissues (percent representation of *Bdnf V* at 1-month: 9.7%, 6-month: 9.4%, and 17-month: 6.2%). By contrast, the other stress-responsive isoform *Bdnf IV* is detected at 1-month and 6-months of age in both male and female ileal LM-MP (percent representation of *Bdnf IV* at 1-month: 5.3%, and 6-month: 2.3%), but it is not detected in the aging ileal LM-MP – suggesting that the expression of this isoform is reduced or lost with aging. On the other hand, the expression of *Bdnf II* (e2) is not detected at 1-month of

312 age but is detected at 6-months and 17-months of age (percent representation of *Bdnf II* at 6-
313 month: 3.3%, and 17-month: 5.1%). 6-months age is the only age we queried where we detected
314 the expression of *Bdnf-III* in the murine ileal LM-MP (representing 2.9% of all *Bdnf* transcripts at
315 this age) (**Extended Fig 3-1**). These data show that stress-responsive *Bdnf* isoforms (*IV* and *VI*)
316 represent about or more than 85% of all *Bdnf* transcripts at any age in the murine ileal myenteric
317 plexus.

318 **BDNF and TrkB are expressed by myenteric neurons.** Prior data have used
319 immunohistochemical and conditional transgenic mice to establish the expression of BDNF in
320 myenteric ganglia in the post-natal gut (Kovler et al., 2021; Singh et al., 2022). The secreted
321 nature of BDNF and the non-inducible conditional animals used for these experiments have thus
322 left open the question about the exact nature of myenteric cells that express this neurotrophin. By
323 contrast, using a reporter transgenic mouse, have previously shown that TrkB is expressed by
324 myenteric neurons in the adult gut (Nestor-Kalinoski et al., 2022). Here, we use RNAScope to test
325 the expression of transcripts of *Bdnf* and *Ntrk2* (TrkB gene) in the adult murine myenteric plexus.
326 By using RNAScope probes for *Bdnf, Ntrk2*, and the pan-neuronally expressed gene *Tubb3* that
327 were hybridized with fresh-frozen sections of the small intestinal LM-MP tissues, we observed
328 that *Bdnf* and *Ntrk2* transcripts were detected in *Tubb3*$^{+}$ enteric neurons (**Fig 4A**). This data shows
329 that *Bdnf* and *Ntrk2* (TrkB) are neuronally expressed genes in the myenteric plexus. We next
330 performed immunohistochemistry on formalin fixed paraffin embedded (FFPE) tissue sections
331 from the adult small intestine of human patients without any known motility disorder and again
332 found that while BDNF protein was present in the myenteric ganglia, its abundance was
333 significantly higher in neuron-like cells. This again suggests that BDNF is a neuronally expressed
334 protein in the adult myenteric ganglia (**Fig 4B**).

335 **Dexamethasone exposure significantly downregulates myenteric BDNF expression**. Since
336 dexamethasone (Dexa), a synthetic glucocorticoid receptor (GR) agonist which mimics the effect
337 of stress-induced increase in cortisol (Dubashynskaya et al., 2021), significantly slows down GI
338 motility (**Fig 2**), we next tested whether exposure to Dexa causes a significant reduction in the
339 expression of stress-responsive *Bdnf IV* and *VI* isoforms. In small intestinal LM-MP of adult male
340 mice treated with Dexa or vehicle, we assessed the abundance of these *Bdnf* at 4 hours post
341 treatment, a timepoint aligning with the duration our WGTT experiments. By performing
342 quantitative real time PCR (qRT-PCR) with isoform-specific TaqMan probes, we found that
343 expression of both *Bdnf IV* and *VI* were significantly reduced in small intestinal LM-MP of mice
344 treated with Dexa when compared to vehicle treated control (n = 3/cohort; mean ± S.E. fold

345 change of *Bdnf IV*: Control: 1.011 ± 0.104; Dexa: 0.536 ± 0.087, p = 0.025; mean ± S.E. fold
346 change of *Bdnf VI*: Control: 1.012 ± 0.110; Dexa: 0.422 ± 0.042, p = 0.007; Students' t-test; **Fig**
347 **5A**).

348 *Bdnf* is an immediate early gene whose expression may be triggered by tissue damage (Ballarín
349 et al., 1991; Hughes et al., 1993). To ensure that our results are not affected by the dissection of
350 tissues immediately before RNA isolation, we cultured peeled adult small intestinal LM-MP tissues
351 from male mice in SCM with vehicle (DMSO) or Dex (1 μM) for 4 hours, and again performed
352 qRT-PCR with *Bdnf* isoform-specific probes. Again, we found that exposure to Dex significantly
353 reduced the expression of both stress responsive isoforms *Bdnf IV* and *Bdnf VI* (n = 3/cohort;
354 mean ± S.E. fold change of *Bdnf IV*: Control: 1.002 ± 0.047; Dexa: 0.510 ± 0.099, p = 0.030;
355 mean ± S.E. fold change of *Bdnf VI*: Control: 1.018 ± 0.140; Dexa: 0.520 ± 0.079, p = 0.028;
356 Students' t-test; **Fig 5B**).

357 Next, we repeated these experiments and used the adult murine small intestinal LM-MP tissues
358 cultured with and without Dex for assessing whether exposure to Dex caused change in BDNF
359 protein levels in tissue. By performing an ELISA, we found that LM-MP cultured with Dex for 4
360 hours showed significant reduction in the levels of BDNF proteins when compared to LM-MP
361 cultured with vehicle (n = 3/cohort; mean ± S.E. BDNF levels (in pg/g of tissue): Control: 473.0 ±
362 45.32; Dexa: 85.5 ± 32.63, p = 0.002; Students' t-test; **Fig 5C**).

363 **Targeted activation of TrkB restores motility in Dex-induced delayed transit models.** Our
364 observations that reduced *Bdnf* expression is associated with slowed whole gut motility in Dexa-
365 treated mice suggests that the effect of Dexa on whole gut motility may be mediated by a reduced
366 BDNF–TrkB signaling. This would suggest that increasing TrkB signaling would improve gut
367 motility of Dexa-treated mice. To test this hypothesis, we studied whether a synthetic and specific
368 agonist of TrkB can restore whole gut motility of Dexa-treated mice. In rodent models, the
369 serotonin-derived compound HIOC has been demonstrated to be a specific agonist of TrkB
370 (Dhakal et al., 2021). We found that cohorts of mice that were pre-treated with HIOC and then
371 treated with Dexa had significantly lower whole gut transit times on average than Dexa-treated
372 mice that were not treated with HIOC (n = 9/cohort; mean ± S.E. of WGTT (in min): Dexa: 228.3

373 ± 7.12; Dexa + HIOC: 150.0 ± 21.94, p = 0.003, Students' t-test; **Fig 5D**). Of note, we find higher
374 variability in the whole gut transit time in the dual-agonist (Dexa + HIOC) cohort compared to
375 Dexa cohort.

376

377 **Discussion**

378 Our study establishes that altered BDNF–TrkB signaling in the adult ENS is an important
379 mechanism through which the stress-induced glucocorticoid pathway manifests GI dysmotility.
380 Our study is the first to interrogate the nature of the *Bdnf* isoforms present in the post-natal gut of
381 juvenile, adult, and aging mice, and establishes that at all ages, the stress-responsive (also the
382 glucocorticoid-responsive) isoform *Bdnf VI* is the dominant *Bdnf* isoform expressed in the gut wall.
383 Further, by demonstrating the localization of *Bdnf* and *Ntrk2* transcripts in *Tubb3*-expressing
384 myenteric neurons in the adult murine gut wall, we show that the BDNF–TrkB crosstalk is neuronal
385 in nature. Since stress downregulates the expression of *Bdnf-IV* and *Bdnf-VI* through a
386 glucocorticoid-mediated mechanism, we tested and found that glucocorticoid receptor (GR)
387 agonism (using a synthetic GR agonist dexamethasone) significantly downregulated BDNF
388 expression in the adult LM-MP, and that this was associated with a significant slowdown of
389 intestinal motility. Finally, we established the involvement of the BDNF–TrkB signaling in
390 glucocorticoid-mediated GI dysmotility by showing that TrkB agonism significantly improves GI
391 motility in a mouse model of dexamethasone-induced GI dysmotility. These results together show
392 that GR agonism, an important downstream effect of physiological stress, significantly reduces
393 the expression of *Bdnf-VI* and *IV* isoforms in a subpopulation of myenteric neurons, which results
394 in reduced TrkB signaling in another subpopulation of myenteric neurons to cause GI dysmotility.
395 Promoting TrkB signaling in myenteric neurons thus holds the key to improving GI motility in
396 stress-induced GI dysmotility conditions.

397 Prior studies have shown that stress and the stress hormone corticotrophin-releasing factor (CRF)
398 in the central nervous system (CNS) induce a slowdown of gastric, small intestinal, and whole gut
399 transit (Zhao et al., 2021; Lobo et al., 2023). Through stimulation of the HPA axis, stress causes
400 increased release of the glucocorticoid cortisol, which has been previously simulated by using the
401 glucocorticoid receptor (GR) agonist dexamethasone. The Thaiss lab demonstrated that GR
402 (*Nr3c1*) is expressed by enteric neurons, and that both stress and dexamethasone similarly slow
403 GI motility (Schneider et al., 2023). Using dexamethasone to simulate the glucocorticoid effect of

404 physiological stress, we identified glucocorticoid-mediated reduction in BDNF–TrkB signaling as
405 a key pathway driving stress-associated GI dysmotility.

406 Alterations and mutations in *Bdnf* and *Ntrk2* have been associated with GI dysmotility (Bonfiglio
407 et al., 2021; Weaver et al., 2022; Linsalata et al., 2023), and exogenous supplementation of BDNF
408 has been observed to have a prokinetic effect in patients (Coulie et al., 2000; Chen et al., 2014).
409 However, the cellular and molecular mechanisms that regulate BDNF levels in these diseases of
410 gut-brain interactions (DGBI) that are often associated with aberrant stress responses were
411 unknown. Our study, which identifies the neuronal nature of BDNF and TrkB and that stress and
412 glucocorticoid-responsive *Bdnf VI* isoform is the most abundant isoform across ages in the post-
413 natal ENS, is the first to establish the mechanism through which this clinically relevant
414 biomolecule is altered in the gut. Previously, the Belgian group (Boesmans et al., 2008) showed
415 that BDNF amplifies neuronal responsiveness of enteric neurons to stimuli, suggesting that this
416 neurotrophin regulates the '*gain*' of TrkB-expressing neurons. These observations, along with our
417 and others' observation of the neuronal nature of TrkB (Boesmans et al., 2008; Nestor-Kalinoski
418 et al., 2022), and our data showing that increasing TrkB signaling in dexamethasone-treated mice
419 improves GI motility suggests that stress-mediated downregulation of BDNF reduces the
420 sensitivity or responsiveness of TrkB-expressing myenteric neurons to cause dysmotility.
421 Together, this identifies that TrkB is an important therapeutic target for the amelioration of GI
422 dysmotility in DGBI patients.

423 It is important to note that while stress-mediated change in glucocorticoid signaling is an important
424 mechanism through which stress manifests dysfunction, stress also drives changes in other
425 hormones in the viscera, which include changes in adrenaline and in the peripheral release of
426 corticotrophin releasing factor (CRF) from mast cells (Kempuraj et al., 2017; Pace and Myers,
427 2023). It is currently unclear how these alternate stress-mediated pathways affect the enteric
428 BDNF–TrkB signaling, and future studies will focus on elucidating this biology further. In addition,
429 our study also identifies important age-associated changes in abundance of *Bdnf* isoforms other
430 than *Bdnf VI*, and future studies will test whether the glucocorticoid-mediated changes in the
431 expression of *Bdnf VI* and other isoforms occurs differentially in an age-associated manner.

432 Thus, by establishing the mechanism through which stress-associated changes in glucocorticoid
433 signaling alters the BDNF–TrkB crosstalk in the adult enteric nervous system, our study provides
434 an important pathway through which stress causes GI dysmotility and provides a putative
435 therapeutic target which can be used for improving GI motility in many DGBI patients.

Transcriptomic Data and Code availability: Transcriptomic Data and Code availability: All the transcriptomic data has been deposited in GEO GSE284108 and the code for analysis is deposited in Github at https://github.com/jaredslosberg/timecourse_lmmp_bulkrnaseq/

Acknowledgements

We acknowledge Dr. Xia Qian (Dept of Pathology, BIDMC) and Mrs. Vilmonse (Eva) Csizmadia (Dept of Anesthesia, BIDMC) for their help. The authors would like to thank the Neurobiology Imaging Facility (NIF) at Harvard Medical School, Boston, MA for performing the RNAscope assay. This work was supported by funding from NIA R01AG66768, R21AG072107, Diacomp Foundation (Pilot award Augusta University) and Pilot grant from the Harvard Digestive Disease Core (SK). This work was also supported by funding from the Maryland Genetics, Epidemiology, and Medicine training program sponsored by the Burroughs Welcome Fund (JS) and from Walter Benjamin Fellowship (528835020) from Deutsche Forschungsgemeinschaft (PS).

449 **Figures:**

450 **Figure 1. Restraint stress significantly increases whole gut transit time in adult male mice.**
451 Graphical representation of the mean ± standard error of the whole gut transit times (assayed
452 using the carmine-red dye method) of two cohorts of mice, where the mice in the 'Stress' cohort
453 were restrained for an hour every day for 5 days, and the 'Control' cohort mice were handled
454 similarly but not restrained. Mice in the Stress cohort showed significantly longer whole gut transit
455 times on average than mice in the control cohort. *$p < 0.05$. Student's t-test.

456 **Figure 2. Dexamethasone treatment significantly increases whole gut transit time in adult**
457 **male mice.** Graphical representation of the mean ± standard error of the whole gut transit times
458 (assayed using the carmine-red dye method) of two cohorts of mice, where the mice in the 'Dexa'
459 cohort were dosed once with dexamethasone (5mg/Kg body weight), and the 'Control' cohort mice
460 were dosed with Vehicle (10% DMSO in Saline). Mice in the Dexa cohort showed significantly
461 longer whole gut transit times on average than mice in the control cohort. *$p < 0.05$. Student's t-
462 test.

463 **Figure 3. *Bdnf VI* is the dominant *Bdnf* isoform in the ileal LM-MP at all post-natal ages.**
464 Graphical representation of the proportions of various *Bdnf* isoforms whose transcripts were
465 detected in the murine ileal LM-MP layer in two different sexes across three different ages of 1-
466 month (juvenile), 6-month (mature adult), and 17-month (aging). This representation shows that
467 stress-responsive *Bdnf VI* is the dominant isoform found in the murine ileal LM-MP at all ages,
468 with its proportions accounting for >80% of all isoforms. The isoform *Bdnf V* is the second most
469 represented isoform at all ages in the murine LM-MP layer but little is known about the
470 mechanisms that regulate its expression. In addition to *Bdnf VI, Bdnf IV* is another stress-
471 responsive isoform detected in the juvenile and adult mice but is not detected in aging murine
472 ileal LM-MP. In contrast to *Bdnf IV, Bdnf II* isoform is detected in the adult and aging ileal tissues,
473 but not in the juvenile tissues. Finally, *Bdnf III* isoform is detected only in the adult ileal LM-MP
474 and not at the other ages.

475 **Extended Figure 3 – 1**: **Gene and isoform expression of *Bdnf* by age**. (A) *Bdnf* expression is
476 detected in 1-month, 6-month, and 17-month-old mice. Isoform-level abundance estimates were
477 collapsed to gene-level after inter-library normalization with edgeR (TMM method). Across all
478 ages, average expression of *Bdnf* is 0.38 ± 0.02 TPM. Independently, gene-level differential
479 expression across age was conducted with DESeq2 (counts ~ age + RIN + batch, Wald test) and
480 *Bdnf* was not identified as differential by age across any comparison. (B) Abundance estimates
481 of individual *Bdnf* isoforms identify the e6 isoform (ENSMUST00000111045) as the majority

482 isoform in each condition. The average expression of this isoform is 0.32 ± 0.08 TPM. Other lowly
483 detected isoforms include e5 (ENSMUST00000176893), e4 (ENSMUST00000111050), e3
484 (ENSMUST00000111046), and e2 (ENSMUST00000111047), while remaining isoforms were not
485 detected. Differential isoform usage by age was tested via the DEXSeq wrapper within
486 IsoformSwitchAnalyzeR (Likelihood ratio test, full model: ~ sample + exon + age:exon, reduced
487 model: ~ sample + exon). No *Bdnf* isoforms were identified as having significant differential usage
488 by age. (C) Isoform level expression was transformed to isoform fraction (IF) measures by age
489 (for each age, sum of IF's is 1).

490 **Figure 4. *Bdnf* is a neuronally expressed gene in the adult murine small intestinal ENS.**
491 Transcriptomic and proteomic evidence of neuronal expression of BDNF. (A) Confocal microscopy
492 image of a 14 µm thick section of adult murine ileal LM-MP tissue which was probed with
493 RNAScope-probes against all *Bdnf* (green), *Ntrk2* (red) transcripts and against the pan-neuronal
494 *Tubb3* (grey) transcript show that off (i, ii) all the *Tubb3*-expressing myenteric neurons, distinct
495 neurons express *Bdnf* (yellow arrow, (i, iii)) and *Ntrk2* (TrkB, red arrow, (i, iv)). That *Bdnf* and *Ntrk2*
496 expressing neurons are distinct neurons can also be observed in (v) an image representation
497 where the dominant *Tubb3* transcripts are not visualized. No other cellular subset inside or outside
498 the ganglia shows expression of *Bdnf* or *Ntrk2* transcripts providing evidence that BDNF and TrkB
499 in the adult small intestine are neuronally restricted. Nuclei are labeled with DAPI (blue). Scale
500 bar represents 10 µm. (B) Immunostaining a human small intestinal tissue section with antibodies
501 against BDNF also shows that while the secreted form of BDNF is present inside and outside of
502 the myenteric ganglia, the highly enriched presence of BDNF in the cytoplasm of a myenteric
503 neuron (black arrow) suggests its likely source of expression. Scale bar represents 100 µm.

504 **Figure 5. Dexamethasone causes a significant reduction in the abundance of enteric BDNF**
505 **to drive GI dysmotility.** (A) Adult male mice dosed with dexamethasone (Dexa) and sacrificed 4
506 hours later showed a significant down regulation in the expression of stress and glucocorticoid-
507 responsive *Bdnf IV* and *Bdnf VI* transcripts in their small intestinal LM-MP tissues, when compared
508 to age- and sex-matched mice that were dosed with vehicle. *$p < 0.05$, **$p < 0.01$, Students' t-
509 test. (B) Small intestinal LM-MP tissues from adult male mice that were cultured with Dexa for 4
510 hours showed a significant down regulation in the expression of stress and glucocorticoid-
511 responsive *Bdnf IV* and *Bdnf VI* transcripts in their small intestinal LM-MP tissues, when compared
512 to tissues from age- and sex-matched mice that were cultured with vehicle. *$p < 0.05$, Students'
513 t-test. (C) Small intestinal LM-MP tissues from adult male mice that were cultured with Dexa for 4

514 hours showed a significant reduction in the abundance of BDNF protein as assessed by ELISA,
515 when compared to tissues from age- and sex-matched mice that were cultured with vehicle. **p
516 < 0.01, Students' t-test. (D) Dexa-treated adult male mice that were also dosed with the synthetic
517 and specific agonist of TrkB HIOS showed significant reduction in their whole gut transit time of
518 orally gavaged carmine-red dye, and hence improved gut motility, when compared to age- and
519 sex-matched mice that were dosed only with Dexa.

520

521 **Table 1**

Resource	Vendor	Cat. No.
BDNF antibody	Abcam	Ab108319
Bdnf RNAScope assay	RNAScope, ACD-Bio	457761
Ntrk2 RNAScope assay	RNAScope, ACD-Bio	423611-C2
Tubb3 RNAScope assay	RNAScope, ACD-Bio	423391-C3
TaqMan Primers & Probes		
Target	**Sequence/Cat. No.**	**Company**
Bdnf IV Fwd	CGTTTACTTCTTTCATGGGCG	IDT
Bdnf IV Rev	AGCTGCCTTGATGTTTACTTTG	IDT
Bdnf IV probe	56-FAM/AGGATGGTC/ZEN/ATCACTCTTCTCACCTGG/3IABkFQ	IDT
Bdnf VI Fwd	ATGCAACCGAAGTATGAAATAACC	IDT
Bdnf VI Rev	GGACCAGAAGCGTGACAAC	IDT
Bdnf VI probe	56-FAM/ACCAGGTGA/ZEN/GAAGAGTGATGACCATCC/3IBkFQ	IDT
Hprt TaqMan assay	Mm00446966_m1	Invitrogen

522

523

524

525

526

527 **References:**

528 Aid T, Kazantseva A, Piirsoo M, Palm K, Timmusk T (2007) Mouse and rat BDNF gene structure
529 and expression revisited. J Neurosci Res 85:525-535.
530 Ballarín M, Ernfors P, Lindefors N, Persson H (1991) Hippocampal damage and kainic acid
531 injection induce a rapid increase in mRNA for BDNF and NGF in the rat brain.
532 Experimental Neurology 114:35-43.
533 Begni V, Riva Marco A, Cattaneo A (2016) Cellular and molecular mechanisms of the brain-
534 derived neurotrophic factor in physiological and pathological conditions. Clinical Science
535 131:123-138.
536 Boesmans W, Gomes P, Janssens J, Tack J, Vanden Berghe P (2008) Brain-derived neurotrophic
537 factor amplifies neurotransmitter responses and promotes synaptic communication in
538 the enteric nervous system. Gut 57:314-322.
539 Bonfiglio F et al. (2021) GWAS of stool frequency provides insights into gastrointestinal motility
540 and irritable bowel syndrome. Cell Genom 1:None.
541 Chalazonitis A, Li Z, Pham TD, Chen J, Rao M, Lindholm P, Saarma M, Lindahl M, Gershon MD
542 (2020) Cerebral dopamine neurotrophic factor is essential for enteric neuronal
543 development, maintenance, and regulation of gastrointestinal transit. J Comp Neurol
544 528:2420-2444.
545 Chen F, Yu Y, Wang P, Dong Y, Wang T, Zuo X, Li Y (2014) Brain-derived neurotrophic factor
546 accelerates gut motility in slow-transit constipation. Acta Physiol (Oxf) 212:226-238.
547 Chen FX, Yu YB, Yuan XM, Zuo XL, Li YQ (2012) Brain-derived neurotrophic factor enhances the
548 contraction of intestinal muscle strips induced by SP and CGRP in mice. Regul Pept
549 178:86-94.
550 Chen H, Lombes M, Le Menuet D (2017) Glucocorticoid receptor represses brain-derived
551 neurotrophic factor expression in neuron-like cells. Mol Brain 10:12.
552 Coulie B, Szarka LA, Camilleri M, Burton DD, McKinzie S, Stambler N, Cedarbaum JM (2000)
553 Recombinant human neurotrophic factors accelerate colonic transit and relieve
554 constipation in humans. Gastroenterology 119:41-50.
555 Dhakal S, He L, Lyuboslavsky P, Sidhu C, Chrenek MA, Sellers JT, Boatright JH, Geisert EE,
556 Setterholm NA, McDonald FE, Iuvone PM (2021) A Tropomycin-Related Kinase B
557 Receptor Activator for the Management of Ocular Blast-Induced Vision Loss. J
558 Neurotrauma 38:2896-2906.
559 Dubashynskaya NV, Bokatyi AN, Skorik YA (2021) Dexamethasone Conjugates: Synthetic
560 Approaches and Medical Prospects. Biomedicines 9.
561 Hill JL, Martinowich K (2016) Activity-dependent signaling: influence on plasticity in circuits
562 controlling fear-related behavior. Curr Opin Neurobiol 36:59-65.
563 Hong EJ, McCord AE, Greenberg ME (2008) A biological function for the neuronal activity-
564 dependent component of Bdnf transcription in the development of cortical inhibition.
565 Neuron 60:610-624.
566 Hughes P, Beilharz E, Gluckman P, Dragunow M (1993) Brain-derived neurotrophic factor is
567 induced as an immediate early gene following N-methyl-d-aspartate receptor activation.
568 Neuroscience 57:319-328.

569 Kempuraj D, Selvakumar GP, Thangavel R, Ahmed ME, Zaheer S, Raikwar SP, Iyer SS, Bhagavan
570 SM, Beladakere-Ramaswamy S, Zaheer A (2017) Mast Cell Activation in Brain Injury,
571 Stress, and Post-traumatic Stress Disorder and Alzheimer's Disease Pathogenesis. Front
572 Neurosci 11:703.
573 Konturek TJ, Martinez C, Niesler B, van der Voort I, Mönnikes H, Stengel A, Goebel-Stengel M
574 (2020) The Role of Brain-Derived Neurotrophic Factor in Irritable Bowel Syndrome. Front
575 Psychiatry 11:531385.
576 Kovler ML, Gonzalez Salazar AJ, Fulton WB, Lu P, Yamaguchi Y, Zhou Q, Sampah M, Ishiyama A,
577 Prindle T, Jr., Wang S, Jia H, Wipf P, Sodhi CP, Hackam DJ (2021) Toll-like receptor 4-
578 mediated enteric glia loss is critical for the development of necrotizing enterocolitis. Sci
579 Transl Med 13:eabg3459.
580 Kulkarni S et al. (2017) Adult enteric nervous system in health is maintained by a dynamic
581 balance between neuronal apoptosis and neurogenesis. Proc Natl Acad Sci U S A
582 114:E3709-e3718.
583 Leigh S-J, Uhlig F, Wilmes L, Sanchez-Diaz P, Gheorghe CE, Goodson MS, Kelley-Loughnane N,
584 Hyland NP, Cryan JF, Clarke G (2023) The impact of acute and chronic stress on
585 gastrointestinal physiology and function: a microbiota–gut–brain axis perspective. The
586 Journal of Physiology 601:4491-4538.
587 Linsalata M, Prospero L, Riezzo G, Orlando A, D'Attoma B, Ignazzi A, Russo F (2023) Somatization
588 is associated with altered serum levels of vitamin D, serotonin, and brain-derived
589 neurotrophic factor in patients with predominant diarrhea irritable bowel syndrome.
590 Neurogastroenterol Motil 35:e14512.
591 Linz R, Puhlmann LMC, Apostolakou F, Mantzou E, Papassotiriou I, Chrousos GP, Engert V, Singer
592 T (2019) Acute psychosocial stress increases serum BDNF levels: an antagonistic relation
593 to cortisol but no group differences after mental training. Neuropsychopharmacology
594 44:1797-1804.
595 Liu S (2018) Neurotrophic factors in enteric physiology and pathophysiology. Neurogastroenterol
596 Motil 30:e13446.
597 Lobo B, Tramullas M, Finger BC, Lomasney KW, Beltran C, Clarke G, Santos J, Hyland NP, Dinan
598 TG, Cryan JF (2023) The Stressed Gut: Region-specific Immune and Neuroplasticity
599 Changes in Response to Chronic Psychosocial Stress. J Neurogastroenterol Motil 29:72-
600 84.
601 Martinowich K, Manji H, Lu B (2007) New insights into BDNF function in depression and anxiety.
602 Nat Neurosci 10:1089-1093.
603 Murakami S, Imbe H, Morikawa Y, Kubo C, Senba E (2005) Chronic stress, as well as acute stress,
604 reduces BDNF mRNA expression in the rat hippocampus but less robustly. Neurosci Res
605 53:129-139.
606 Nestor-Kalinoski A, Smith-Edwards KM, Meerschaert K, Margiotta JF, Rajwa B, Davis BM, Howard
607 MJ (2022) Unique Neural Circuit Connectivity of Mouse Proximal, Middle, and Distal
608 Colon Defines Regional Colonic Motor Patterns. Cell Mol Gastroenterol Hepatol 13:309-
609 337.e303.
610 Pace SA, Myers B (2023) Hindbrain Adrenergic/Noradrenergic Control of Integrated Endocrine
611 and Autonomic Stress Responses. Endocrinology 165.

612 Pruunsild P, Sepp M, Orav E, Koppel I, Timmusk T (2011) Identification of cis-elements and
613 transcription factors regulating neuronal activity-dependent transcription of human
614 BDNF gene. J Neurosci 31:3295-3308.
615 Qin HY, Cheng CW, Tang XD, Bian ZX (2014) Impact of psychological stress on irritable bowel
616 syndrome. World J Gastroenterol 20:14126-14131.
617 Russell G, Lightman S (2019) The human stress response. Nature Reviews Endocrinology 15:525-
618 534.
619 Schneider KM et al. (2023) The enteric nervous system relays psychological stress to intestinal
620 inflammation. Cell 186:2823-2838.e2820.
621 Sharkey KA, Mawe GM (2023) The enteric nervous system. Physiol Rev 103:1487-1564.
622 Singh A, Singh J, Rattan S (2022) Evidence for the presence and release of BDNF in the neuronal
623 and non-neuronal structures of the internal anal sphincter. Neurogastroenterology &
624 Motility 34:e14099.
625 Singh A, Mohanty I, Singh J, Rattan S (2020) BDNF augments rat internal anal sphincter smooth
626 muscle tone via RhoA/ROCK signaling and nonadrenergic noncholinergic relaxation via
627 increased NO release. Am J Physiol Gastrointest Liver Physiol 318:G23-g33.
628 Sperber AD et al. (2021) Worldwide Prevalence and Burden of Functional Gastrointestinal
629 Disorders, Results of Rome Foundation Global Study. Gastroenterology 160:99-114.e113.
630 Tsankova NM, Berton O, Renthal W, Kumar A, Neve RL, Nestler EJ (2006) Sustained hippocampal
631 chromatin regulation in a mouse model of depression and antidepressant action. Nat
632 Neurosci 9:519-525.
633 Wang F, Flanagan J, Su N, Wang LC, Bui S, Nielson A, Wu X, Vo HT, Ma XJ, Luo Y (2012)
634 RNAscope: a novel in situ RNA analysis platform for formalin-fixed, paraffin-embedded
635 tissues. J Mol Diagn 14:22-29.
636 Weaver KR, Mustapic M, Kapogiannis D, Henderson WA (2022) Neuronal-enriched extracellular
637 vesicles in individuals with IBS: A pilot study of COMT and BDNF. Neurogastroenterol
638 Motil 34:e14257.
639 Wood JD (2016) Enteric Nervous System: Neuropathic Gastrointestinal Motility. Digestive
640 Diseases and Sciences 61:1803-1816.
641 Zhang Y, Bi YX, Chen J, Li S, Wu XX, Zhang L, Lin ZJ, Han S, Ding SZ (2021) Association of
642 Peroxiredoxin 1 and brain-derived neurotrophic factor serum levels with depression and
643 anxiety symptoms in patients with irritable bowel syndrome. Gen Hosp Psychiatry 68:59-
644 64.
645 Zhao Y-X, Cui C-X, Gao J-H, Liu J, Liu Q, Lu F-Y, Xin J-J, Yu X-C, Zhu B (2021) Electroacupuncture
646 ameliorates corticotrophin-releasing factor-induced jejunal dysmotility in a rat model of
647 stress. Acupuncture in Medicine 39:135-145.
648 Zheng Z, Liu Y, Mu R, Guo X, Feng Y, Guo C, Yang L, Qiu W, Zhang Q, Yang W, Dong Z, Qiu S, Dong
649 Y, Cui Y (2024) A small population of stress-responsive neurons in the hypothalamus-
650 habenula circuit mediates development of depression-like behavior in mice. Neuron.

651

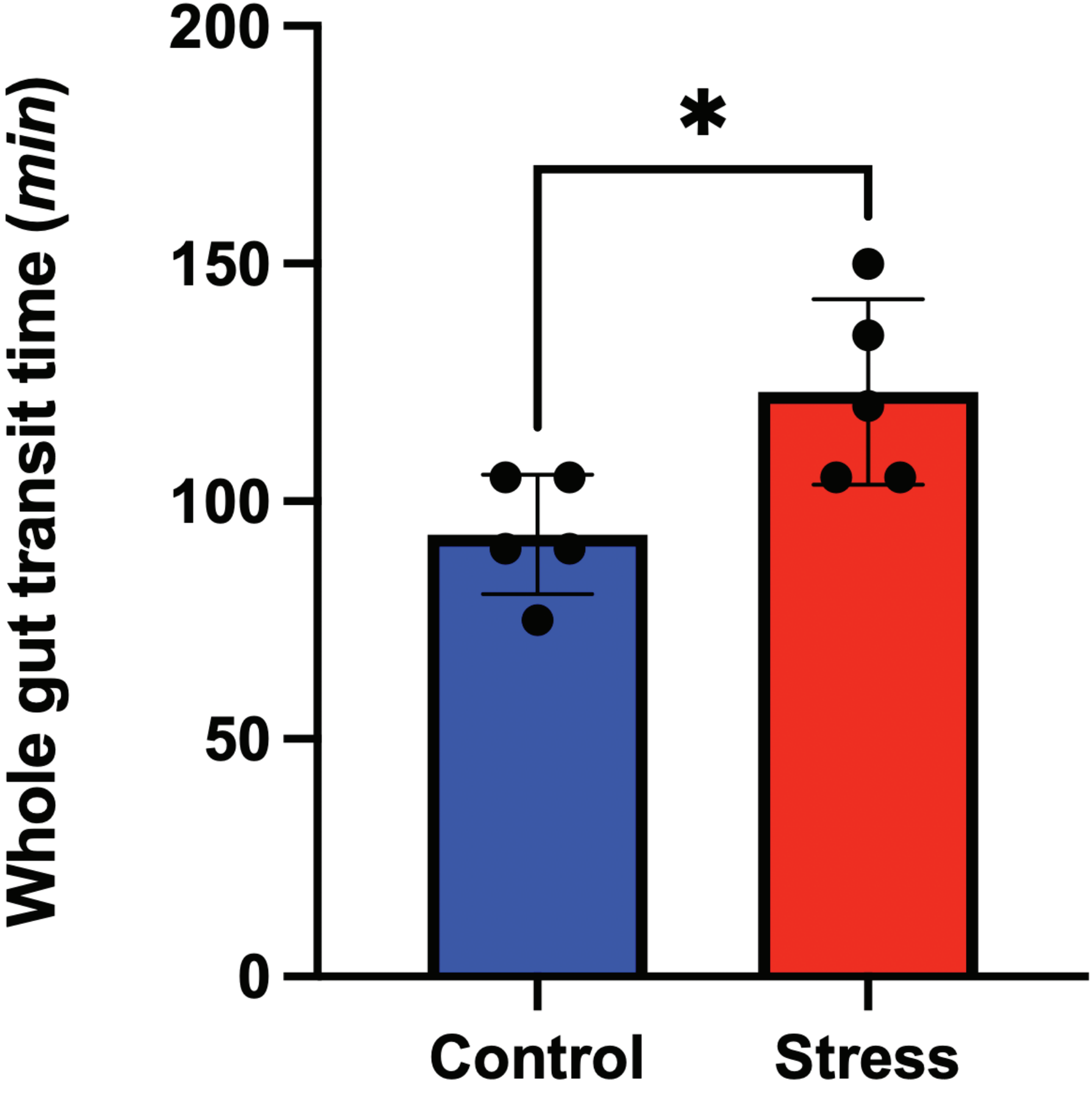
Whole gut transit time (min)
200
150
100
50
0
*
Control
Stress

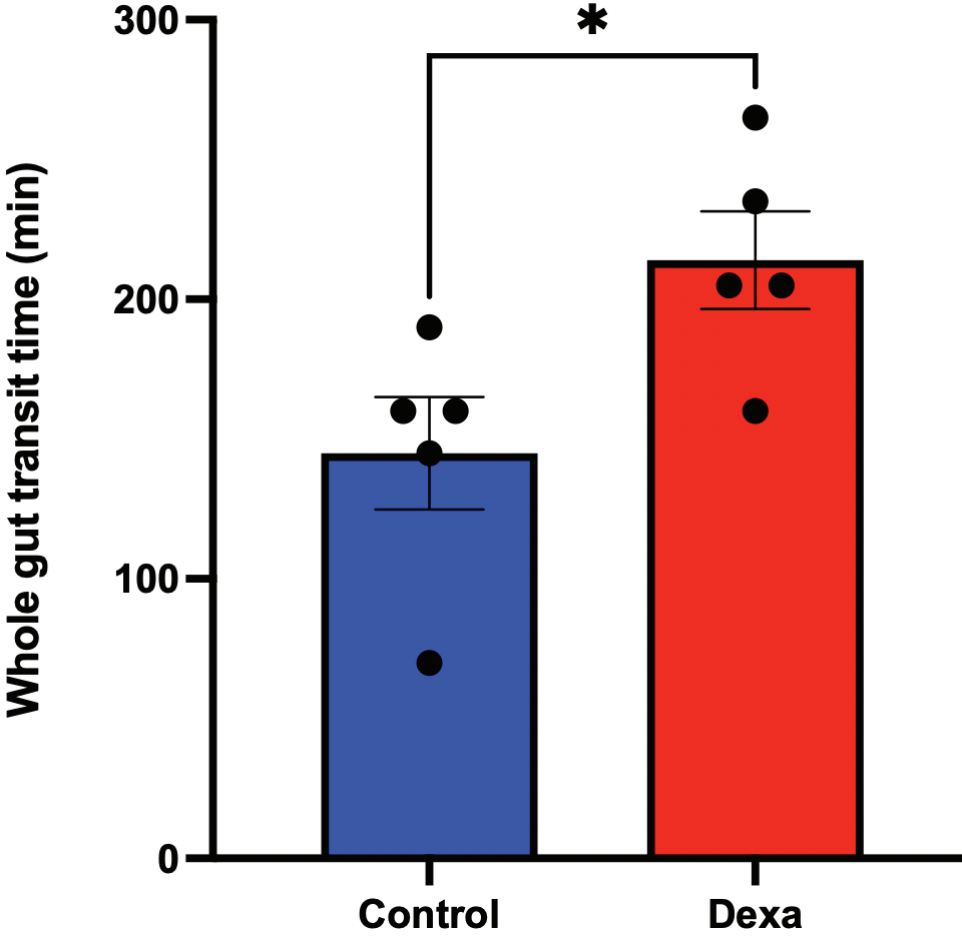
*
300
200
100
0
Whole gut transit time (min)
Control
Dexa

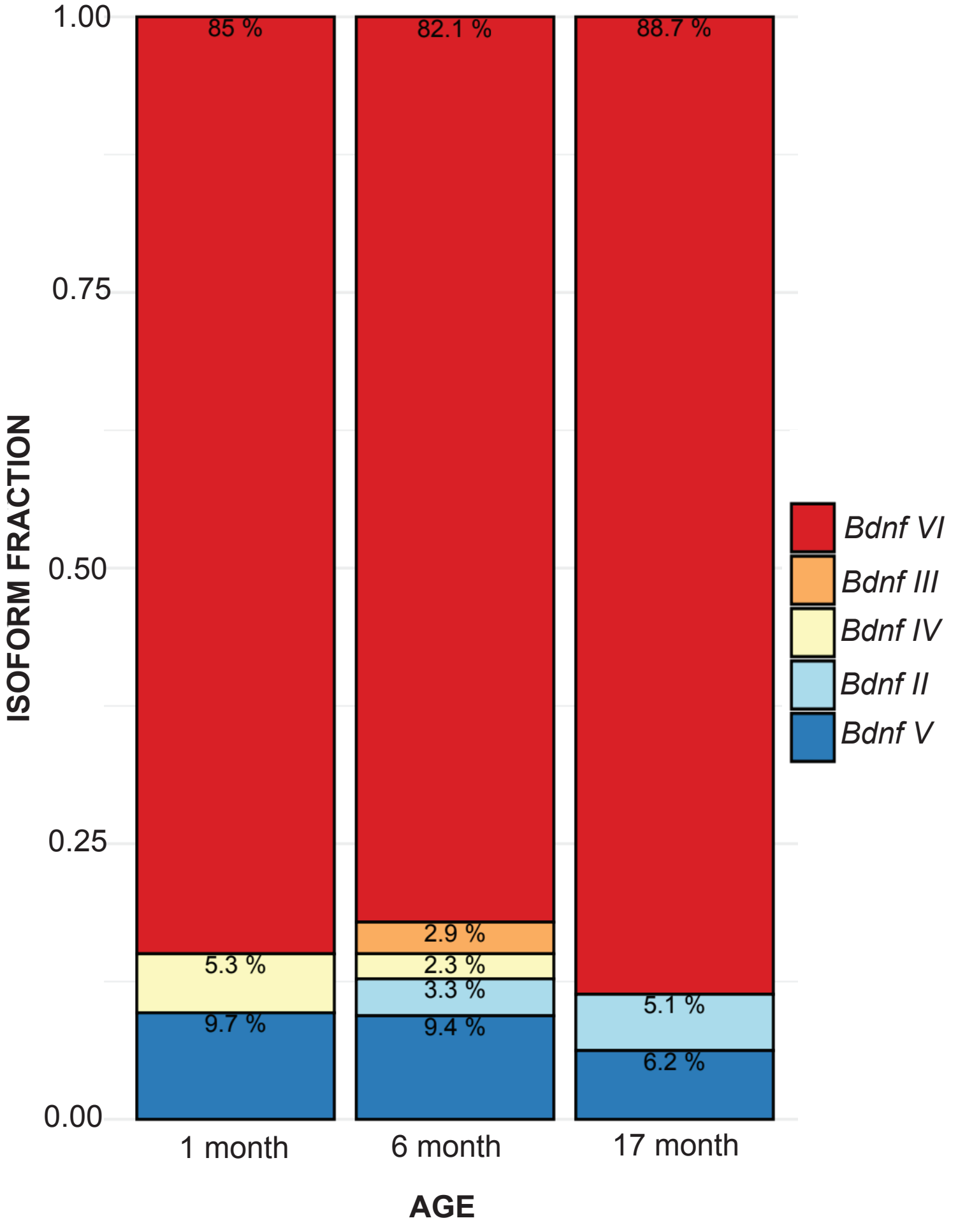
1.00
0.75
0.50
0.25
0.00
ISOFORM FRACTION
85 %
82.1 %
88.7 %
5.3 %
9.7 %
2.9 %
2.3 %
3.3 %
9.4 %
5.1 %
6.2 %
1 month
6 month
17 month
AGE
Bdnf VI
Bdnf III
Bdnf IV
Bdnf II
Bdnf V

1 month 6 month 17 month

AGE

A

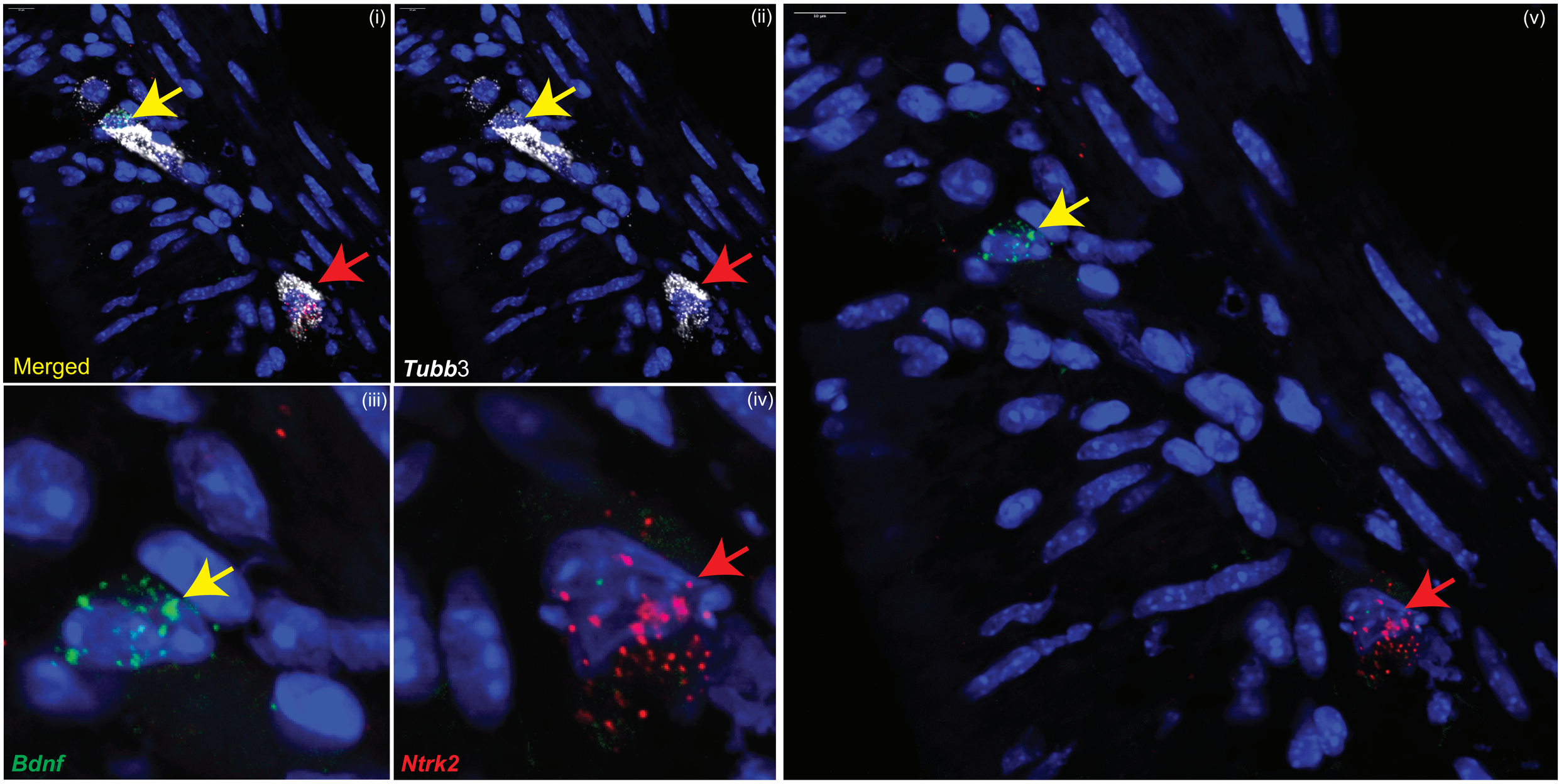

B

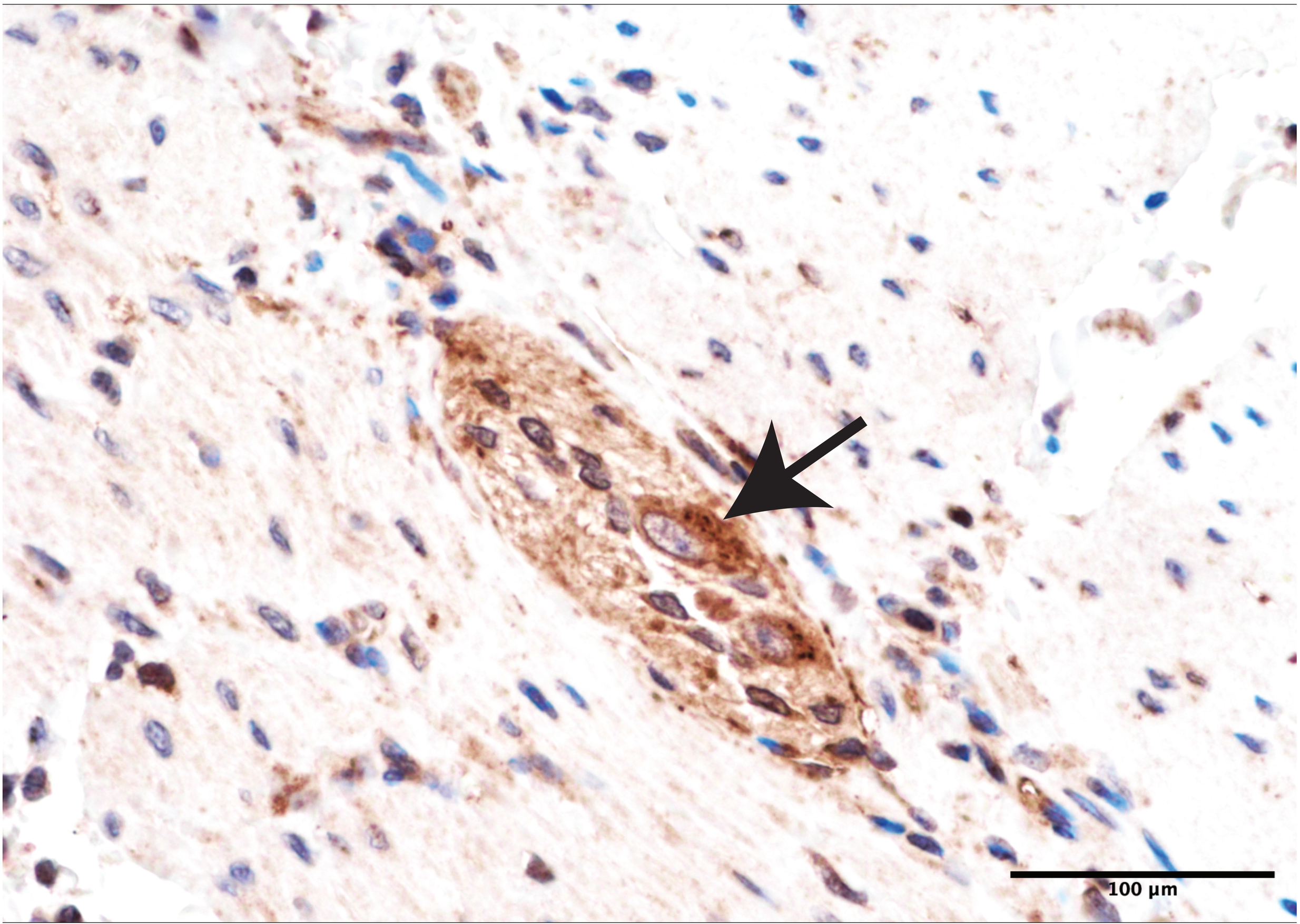

A

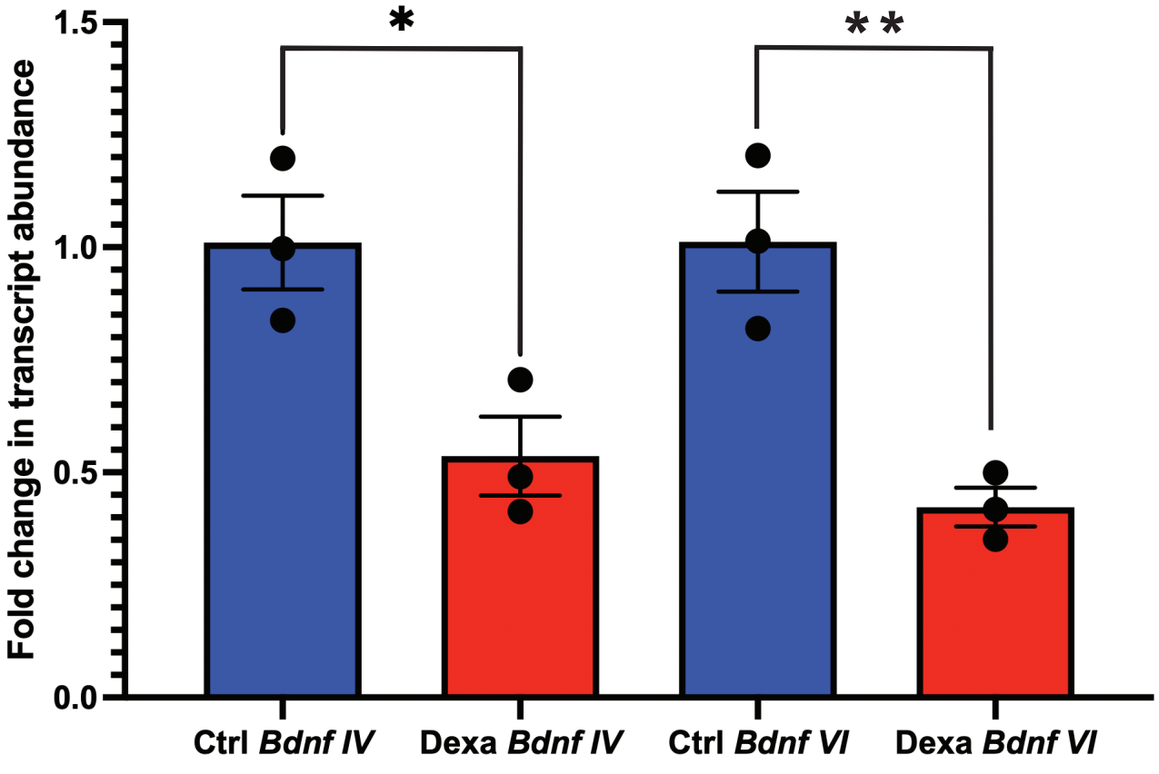
Fold change in transcript abundance
1.5
1.0
0.5
0.0
*
**
Ctrl *Bdnf IV*
Dexa *Bdnf IV*
Ctrl *Bdnf VI*
Dexa *Bdnf VI*

B

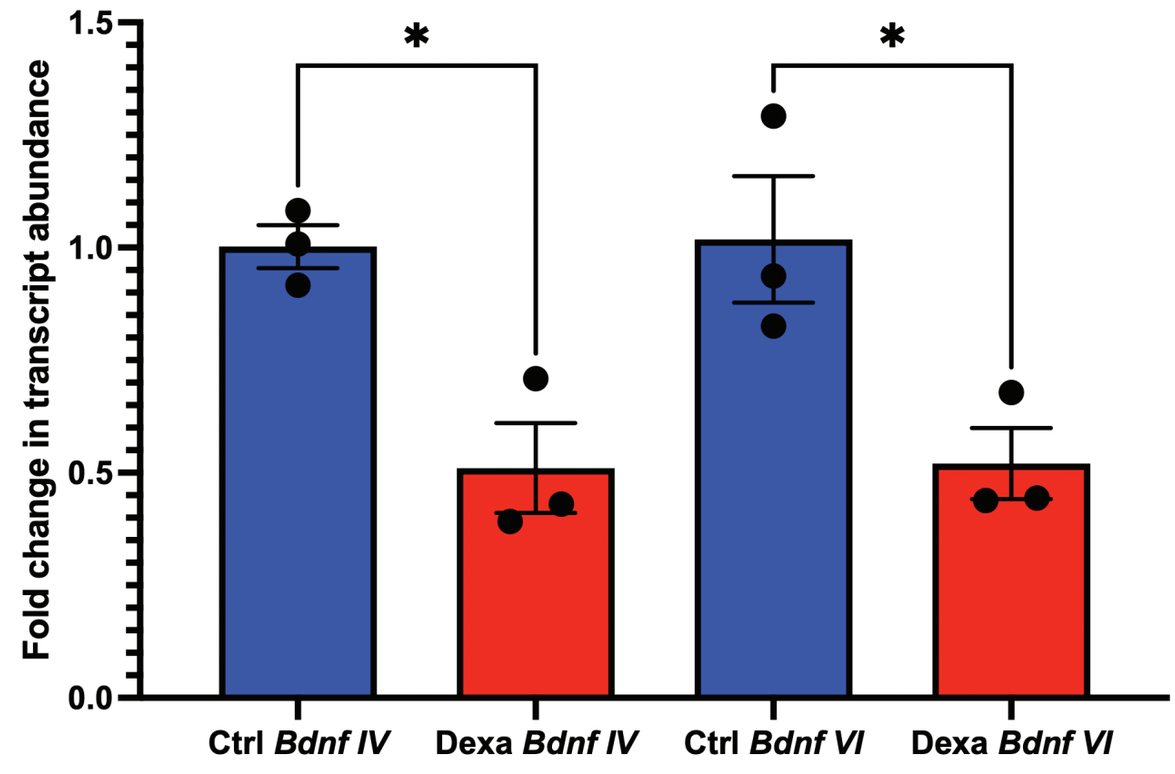
Fold change in transcript abundance
1.5
1.0
0.5
0.0
*
*
Ctrl *Bdnf IV*
Dexa *Bdnf IV*
Ctrl *Bdnf VI*
Dexa *Bdnf VI*

C

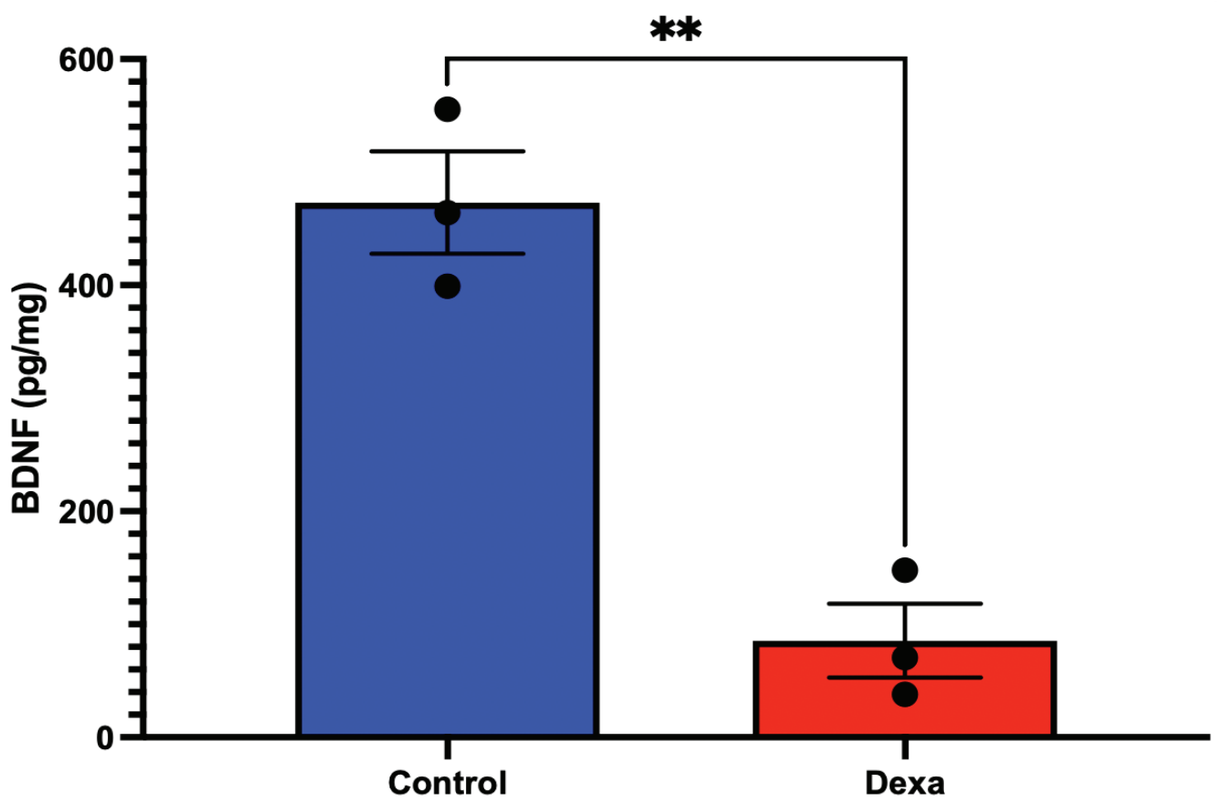
BDNF (pg/mg)
600
400
200
0
**
Control
Dexa

D

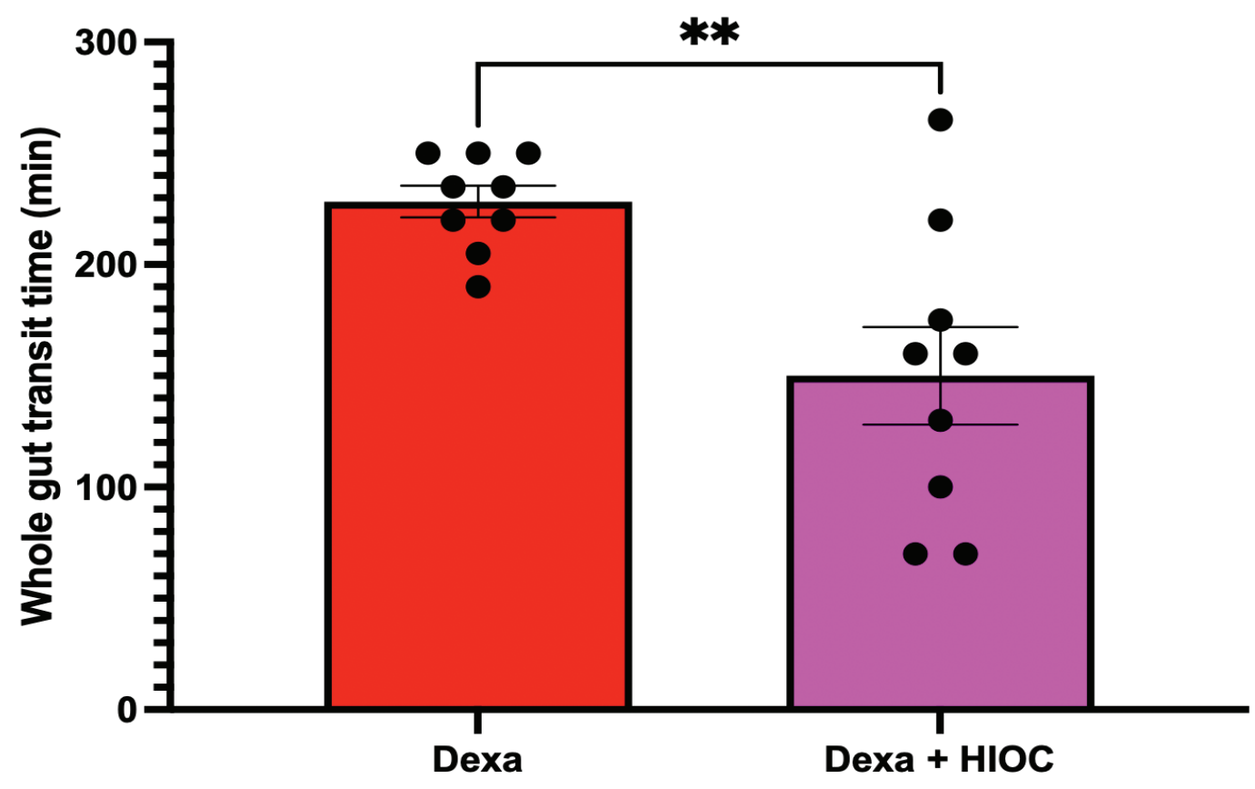
Whole gut transit time (min)
300
200
100
0
**
Dexa
Dexa + HIOC